

Cite this: *RSC Adv.*, 2017, 7, 28661

# Tailoring chain structures of L-lactide and $\epsilon$ -caprolactone copolyester macromonomers using *rac*-binaphthyl-diyl hydrogen phosphate-catalyzed ring-opening copolymerization with monomer addition strategy†

Yanjiao Wang,<sup>a</sup> Ming Xia,<sup>b</sup> Xueqiang Kong,<sup>b</sup> Steven John Severtson<sup>\*c</sup>  
and Wen-Jun Wang<sup>id</sup> <sup>\*a</sup>

Copolymerizations involving polyester macromonomers (MMs) generated from biomass provide a new route for introducing high biomass content into existing polymeric products. Stannous 2-ethylhexanoate-catalyzed ring-opening copolymerization (ROCoP) is commonly utilized to synthesize MMs, but this approach generates polymer chains containing terminal metal residues and limits control of MM chain structures due to the presence of transesterification side reactions (TSRs). Here, *rac*-1,1'-binaphthyl-2,2'-diyl-hydrogenphosphate (*rac*-BNPH) was used for the 2-hydroxyethyl methacrylate (HEMA) initiated ROCoP of L-lactide (L-LA) and  $\epsilon$ -caprolactone ( $\epsilon$ -CL) to produce the well-defined MMs. The copolymerization kinetics and monomer feeding strategies, batch and semibatch, were studied, and the influence on MM chain structures was investigated using both  $^1\text{H}$  and  $^{13}\text{C}$  NMR analysis. The *rac*-BNPH was identified as an effective catalyst for the ROCoP of L-LA and  $\epsilon$ -CL, producing narrowly dispersed MMs with a 96% retention of terminal vinyl groups associated with HEMA. The  $\epsilon$ -CL was more reactive than L-LA, and the reactions exhibited characteristics of living polymerization. The TSRs could be significantly suppressed using batch operation or semibatch with fast  $\epsilon$ -CL addition. It was found that slowing the  $\epsilon$ -CL addition generated more randomly and uniformly distributed comonomers along MM chains. In general, it is demonstrated here that the *rac*-BNPH catalyzed semibatch ROCoPs is an effective means for tailoring the chain structures of MMs.

Received 16th May 2017

Accepted 19th May 2017

DOI: 10.1039/c7ra05531e

rsc.li/rsc-advances

## Introduction

Polyesters have been used in a wide variety of products due to their excellent mechanical properties, weather and corrosion resistance, and ease of processing. Polyesters generated from biomass such as lactide are renewable and biodegradable making them well-suited for disposable packaging and garments.<sup>1,2</sup> They are also nontoxic and biocompatible which qualifies them for biomedical applications.<sup>3,4</sup> More recently, an

approach was introduced for increasing the biomass content in polymeric products by incorporating polyester grafts into polymers composed of acrylic backbones.<sup>5–8</sup> This is achieved most commonly by growing polyester chains on initiators possessing a reactive terminal vinyl group through catalyzed ring-opening polymerizations (ROPs) to generate macromonomers, MMs. The MMs are then polymerized with other monomers to produce the polymers possessing polyester side chains. This approach opens a new route to convert a number of existing commodity products into more sustainable forms.

Previous work on these hybrid materials demonstrates their promise. Ishimoto *et al.*<sup>5</sup> used 2-hydroxyethyl methacrylate, HEMA, as initiator to synthesize MMs with L-lactide, L-LA, containing approximately six lactidyl units. The MMs were then copolymerized with *n*-butyl methacrylate (BMA) using mini-emulsion polymerizations to generate PBMA-*g*-PLLA. Films cast from the formed latexes were reported to demonstrate good elastic properties. In their subsequent work, Ishimoto *et al.* utilized renewable itaconic anhydride (IAN) to generate PLLA graft copolymers using the MM approach as well as a copolymer approach in which PLLA chains are generated on a polymer containing IAN repeat units. Both approaches resulted in

<sup>a</sup>State Key Laboratory of Chemical Engineering, College of Chemical and Biological Engineering, Zhejiang University, Hangzhou, China 310027. E-mail: wenjunwang@zju.edu.cn; Fax: +86-571-8795-2772; Tel: +86-571-8795-2772

<sup>b</sup>Department of Chemistry, Zhejiang University, Hangzhou 310027, China 310027

<sup>c</sup>Department of Bioproducts and Biosystems Engineering, University of Minnesota, Saint Paul, Minnesota, USA 55108. E-mail: sever018@umn.edu; Fax: +1-612-624-3005; Tel: +1-612-625-5265

† Electronic supplementary information (ESI) available: Details about synthesis procedure of L-LA and  $\epsilon$ -CL homo- and block macromonomers and their  $^1\text{H}$  and  $^{13}\text{C}$  NMR spectra and peak assignments,  $^1\text{H}$  NMR spectra for macromonomers of Runs B8, B5, SB1, and SB2, chemical shift assignments of carbonyl carbon sequences in macromonomers, and spin-lattice relaxation time ( $T_1$ ) for carbonyl carbons in  $^{13}\text{C}$  NMR spectrum of macromonomer. See DOI: 10.1039/c7ra05531e

materials that could be further optimized for plastic applications. The synthesis of PLLA MMs having 2 to 20 repeat units with various hydroxyalkyl methacrylates (HAA) initiators including HEMA, 2-hydroxyethyl acrylate (HEA), hydroxypropyl methacrylate (HPMA), and 4-hydroxybutyl acrylate (HBA) were also reported.<sup>9</sup> The MMs were further copolymerized with HAA in solution to produce PHAA-g-PLLA copolymers, which were applied as scaffolding materials for tissue engineering applications. A more immediate application of these materials was demonstrated by Severtson *et al.*<sup>10,11</sup> In order to tailor the thermal properties of the polyester MMs,  $\epsilon$ -caprolactone,  $\epsilon$ -CL, was copolymerized with L-LA to manipulate glass transition temperatures ( $T_g$ s) of formed MMs with HEMA as initiator. The MMs having low  $T_g$  values were then used to replace the acrylic soft monomer in miniemulsion polymerizations to generate pressure-sensitive adhesive (PSA) latexes containing 50 wt% MMs, which provided equivalent and often superior adhesive properties to commercial latex products. It was also demonstrated that the MM composition and chain length could be used to engineer adhesive properties. The use of the MMs approach was further extended for the production of thermoplastic adhesive materials. Much of the 2-ethylhexylacrylate (EHA) was replaced in a commercial acrylic hot-melt formulation with MMs synthesized from the hydroxyl ethylacrylamide initiated copolymerization of L-LA and  $\epsilon$ -CL. The hot-melt adhesives containing 50 wt% MM possessed excellent adhesive properties. In general, the MM approach provides a path forward for synthesizing a broad array of polymer materials with high biomass contents.

The MMs discussed above were synthesized using stannous 2-ethylhexanoate,  $\text{Sn}(\text{Oct})_2$ , catalyzed ROP.  $\text{Sn}(\text{Oct})_2$  is suitable for L-LA homopolymerizations and copolymerizations.<sup>12–15</sup> Although widely used in ROP to prepare polyesters, metal-based catalysts possess complex structures and become bound to generated polymers.<sup>16,17</sup> This inhibits or prevents their removal from polymer products, limiting applications for the generated polymers. Furthermore, metal-catalyzed ring-opening copolymerizations, ROCoPs, are typically accompanied by transesterification side reactions, TSRs.<sup>18</sup> In generating MMs, such reactions limit the control of chain structure and chain length.<sup>13</sup> They also promote the formation of cyclic units<sup>13</sup> and MMs containing two vinyl initiator heads, which act as a crosslinker during the subsequent copolymerization of MM with vinyl monomers. Thus, the preparation of well-defined MMs, with predictable chain structures and chain lengths, requires that TSRs be minimized.

Recently, there has been significant interest in the use of metal-free organocatalysts for making polyesters. Such catalysts are relatively easy to generate and remove from end-products.<sup>19–22</sup> The organocatalysts include organic acid,<sup>23–25</sup> phosphazene,<sup>26,27</sup> pyridine and carbene bases,<sup>28–31</sup> thiourea/amine complex,<sup>32,33</sup> and amidine/guanidine.<sup>34</sup> Hedrick *et al.*<sup>35</sup> was the first to report the successful catalysis of LA ROPs using strongly basic amines, 4-(dimethylamino)pyridine and 4-pyrrolidino-pyridine. The nucleophilic alkali catalysts, in particular carbene bases, have been found to be effective in polymerizing lactone, epoxide, and carbonic anhydride.<sup>17,29</sup> Carbene bases were found to catalyze zwitterionic ROP of cyclic esters in the absence of an alcohol initiator.<sup>36</sup> The guanidine/amidine based catalysts, such

as 1,5,7-triazabicyclo[4.4.0]dec-5-ene (TBD),<sup>37–40</sup> *N*-methyl-TBD,<sup>41</sup> and 1,8-diazabicyclo[5.4.0]undec-7-ene<sup>32</sup> were also effective in catalyzing ROP of LA,  $\delta$ -valerolactone, and  $\epsilon$ -CL, and they demonstrated high activity in catalyzing LA polymerization in nonpolar solvents. Among the organocatalysts, simple organic acids such as 1,1'-binaphthyl-2,2'-diyl-hydrogenphosphate, BNPH, were found to possess high activities in catalyzing the ROP of cyclic monoesters.<sup>19–21</sup> It was reported that the chiral (*R*)-BNPH was used for ROCoP of  $\epsilon$ -CL and LA, but with very low LA incorporation in the copolymer.<sup>21</sup>

Although various organocatalysts have been found to promote ROPs, most of them are ineffective when it comes to catalyzing copolymerizations of ester monomers.<sup>42</sup> Here, efforts to identify alternative catalyst for producing the HEMA initiated L-LA/ $\epsilon$ -CL copolymer MMs through catalyzed ROCoPs are reviewed. The focus is on finding an organocatalyst that is easier to produce, use, and remove once the reaction is complete. As will be discussed, *rac*-BNPH appears to be a promising candidate for the generation of MMs containing L-LA and  $\epsilon$ -CL. To the best of our knowledge, this is the first report of successful reactions for this system. The copolymerization kinetics including transesterification using different monomer feed strategies were studied. The effect of feeding strategies on the control of MM chain structures was also demonstrated.

## Experimental section

### Materials

The L-LA was purchased from Shenzhen Bright China Industrial Co. Ltd. The  $\epsilon$ -CL, HEMA,  $\text{Sn}(\text{Oct})_2$ , *rac*-BNPH, hexane, and hydroquinone were obtained from Sigma Aldrich (St. Louis, MO) and used as received. Deuterated chloroform ( $\text{CDCl}_3$ ) and tetrahydrofuran (THF) were both purchased from J&K China Chemical, Ltd.

### Synthesis of macromonomers

Macromonomers were synthesized with a fixed molar ratio of HEMA/L-LA/ $\epsilon$ -CL = 1/5/4 at a variety of temperatures and polymerization times. Prior to the bulk ROCoPs, reactants were heated and stirred continuously in a round-bottom flask, and the contents were purged with nitrogen gas for approximately 10 min. The flask was then sealed and lowered into a hot oil bath and the contents were heated to the polymerization temperature prior to the addition of 0.5 mol% catalyst using a syringe. Temperature was maintained during the copolymerization under constant mechanical stirring. For copolymerizations involving semibatch operation with monomer addition,  $\epsilon$ -CL (neat) was continuously introduced to the flask at rates of 0.0187 or 0.0468 mol h<sup>−1</sup>, respectively, using a syringe pump. Subsequent to copolymerizations, the flask and contents were cooled and washed with hexane twice to eliminate residual reactants, and the MMs were dried at room temperature in a vacuum oven for 24 h.

### Characterization of macromonomers

Monomer conversions were determined with <sup>1</sup>H nuclear magnetic resonance (NMR) analysis using a Bruker Advance III



operated at 500 MHz. The MMs were dissolved in  $\text{CDCl}_3$  and tetramethylsilane (TMS) was added as the internal standard. All  $^1\text{H}$  NMR spectra were obtained with 512 scans and a 1 s acquisition time. In order to analyze the chain structures, the  $^{13}\text{C}$  NMR spectra of MMs were recorded at 125 MHz with the same spectrometer as used to conduct proton NMR measurements. The carbonyl carbon signals located between 165 and 175 ppm of the  $^{13}\text{C}$  NMR spectra were used for quantitative analysis. Spin-lattice relaxation times ( $T_1$ ) of carbonyl carbons in this range were determined (see ESI†). As  $T_1$  values for all carbonyl carbons used for sequential structure analysis are less than 3.628 s at present conditions, a delay time between pulses of 30 s was used to eliminate the saturation effect. Data were acquired using an acquisition time of 0.865 s, pulse width of 10.5  $\mu\text{s}$ , and a spectral width of 300 ppm. Molecular weights and polydispersity indexes ( $\bar{D}$ ) of macromonomers were characterized using a Waters 1525/2414 Gel Permeation Chromatograph (GPC) equipped with a Waters 2414 differential refractive index detector. THF was used as the eluent at 1.0  $\text{mL min}^{-1}$ . The reported molecular weights and  $\bar{D}$  values are relative to polystyrene standards.

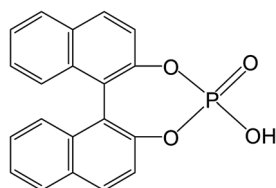
## Results and discussion

### Batch copolymerization of L-LA/ $\epsilon$ -CL using *rac*-BNPH

Along with  $\text{Sn}(\text{Oct})_2$ , which was used in previous studies,<sup>6,7,12,13</sup> *rac*-BNPH (Scheme 1) was used for copolymerization initiated by HEMA at 100 °C with the HEMA/L-LA/ $\epsilon$ -CL molar ratio of 1/5/4. The conversions of L-LA ( $x_{\text{LA}}$ ) and  $\epsilon$ -CL ( $x_{\text{CL}}$ ) at polymerization times of 1, 3, and 7 hours are summarized in Table 1.

The results show significant differences between the catalysts, not only in the general activity they induce but also in their ability to catalyze the ROCoPs of L-LA and  $\epsilon$ -CL. In copolymerization catalyzed by *rac*-BNPH,  $\epsilon$ -CL initially reacted much faster than the L-LA. As the polymerization time was extended, the L-LA was converted. The observation that in *rac*-BNPH catalyzed ROCoPs, L-LA reactivity is less than that of  $\epsilon$ -CL is opposite of that found when the same copolymerization is catalyzed with  $\text{Sn}(\text{Oct})_2$ . But the reactivity of L-LA is much higher than when solution ROCoPs are catalyzed with (*R*)-BNPH in toluene.<sup>21</sup> It was reported that a little L-LA participated in copolymerizations with  $\epsilon$ -CL, even with extended copolymerization times.<sup>21</sup> Our results indicate that *rac*-BNPH shows promise for controlling the ROCoP of L-LA and  $\epsilon$ -CL.

To explore the possibility of enhancing L-LA incorporation rates in *rac*-BNPH catalyzed copolymerizations, ROCoPs were conducted at increasing temperatures up to 160 °C. Table 2 lists characterization data for MMs generated in 7 h reactions



Scheme 1 *rac*-BNPH as organocatalyst for ROCoP of L-LA and  $\epsilon$ -CL.

Table 1 Monomer conversions for bulk ROCoP of L-LA and  $\epsilon$ -CL initiated by HEMA in batch operation using *rac*-BNPH and  $\text{Sn}(\text{Oct})_2$ <sup>a</sup>

Run	Catalyst	$t = 1 \text{ h}$		$t = 3 \text{ h}$		$t = 7 \text{ h}$	
		$x_{\text{LA}}$ (%)	$x_{\text{CL}}$ (%)	$x_{\text{LA}}$ (%)	$x_{\text{CL}}$ (%)	$x_{\text{LA}}$ (%)	$x_{\text{CL}}$ (%)
B1	<i>rac</i> -BNPH	28.6	88.2	40.6	94.9	48.9	98.5
B2	$\text{Sn}(\text{Oct})_2$	77.0	11.0	97.0	37.5	~100	78.7

<sup>a</sup> Molar ratio of HEMA/L-LA/ $\epsilon$ -CL = 1/5/4, polymerization temperature ( $T$ ) = 100 °C, 0.5 mol% (based on the monomer) catalyst,  $t$  denotes reaction time.

including comonomer compositions, % HEMA vinyl group retentions ( $R_v$ ), number-average molecular weights ( $M_n$ ), and polydispersity index values ( $\bar{D}$ ). Raising temperature significantly increased monomer conversions, especially for L-LA. At 160 °C, the L-LA reached nearly full conversion in the 7 h polymerization. During the preparation of the MM, a certain amount of HEMA is expected to polymerize. For copolymerization temperatures greater than 140 °C, the preserved MM terminal vinyl groups from HEMA,  $R_v$ , dropped to about 90%. Reactions between formed MM are expected to form structures that are much larger than target structures based on molar ratios. Furthermore, it is expected that TSRs, which increase the chain disparity, are greatly enhanced at the higher temperatures. The influence of these processes is apparent from values for  $\bar{D}$  with increasing temperature. For example, comparing polymerizations carried out at 160 and 100 °C,  $\bar{D}$  increased from 1.33 to 2.63, respectively. This increase can be limited through the use of paradiox-ybenzene inhibitor, which protects the HEMA double bond. The addition of 0.1 mol% (based on monomers) to copolymerizations carried out at 160 °C lowered the  $\bar{D}$  from 2.63 to 1.85, and 96% of terminal vinyl groups in HEMA were preserved in the MM as opposed to 91% in the absence of the inhibitor.

### *rac*-BNPH catalyzed semibatch bulk copolymerization of L-LA/ $\epsilon$ -CL

The HEMA initiated ROCoP of L-LA and  $\epsilon$ -CL is effectively catalyzed with *rac*-BNPH, but the balance between polymerization rates and the desired chain length parity requires elevated temperatures, e.g., 140 °C, along with use of an inhibitor. The rapid incorporation of  $\epsilon$ -CL relative to L-LA, can be countered through effective monomer feed strategies in semibatch operations. The  $\epsilon$ -CL is better suited for continuous feed operations because it is a liquid at room temperature, while L-LA is in its solid form. Two *rac*-BNPH catalyzed semibatch runs with  $\epsilon$ -CL feeding rates of 0.0468  $\text{mol h}^{-1}$  (SB1) and 0.0187  $\text{mol h}^{-1}$  (SB2) were conducted at 140 °C, and the results are summarized in Table 3. Results for batch runs catalyzed with both *rac*-BNPH and  $\text{Sn}(\text{Oct})_2$  at the same polymerization temperature are also reported in the table for comparison. The conversion of L-LA is increased significantly with the semibatch process involving the continuous feeding of  $\epsilon$ -CL. Nearly complete conversion of the L-LA was obtained for the 0.0187  $\text{mol h}^{-1}$  feed rate. This occurs without the large increase in  $\bar{D}$  observed under semibatch operations.



Table 2 Characterization data for *rac*-BNPH catalyzed bulk ROCoP of L-LA and  $\epsilon$ -CL at various temperatures<sup>a</sup>

Run	<i>T</i> (°C)	<i>x</i> <sub>LA</sub> (%)	<i>x</i> <sub>CL</sub> (%)	<i>R</i> <sub>v</sub> <sup>b</sup> (%)	HEMA/L-LA/ $\epsilon$ -CL <sup>c</sup>	<i>M</i> <sub>n</sub> <sup>NMR</sup> (kg mol <sup>-1</sup> )	<i>M</i> <sub>n</sub> <sup>GPC</sup> (kg mol <sup>-1</sup> )	<i>D</i> <sup>GPC</sup>
B1	100	48.9	98.5	98	1/4.67/4.06	0.89	1.12	1.33
B3	120	73.6	~100	96	1/7.38/4.34	1.11	1.39	1.45
B4	140	92.4	~100	93	1/11.75/5.39	1.59	1.70	1.46
B5 <sup>d</sup>	140	92.7	~100	96	1/9.20/4.28	1.28	1.44	1.43
B6	160	~100	~100	91	1/14.01/5.98	1.95	1.71	2.63
B7 <sup>d</sup>	160	~100	~100	96	1/10.67/4.41	1.36	1.56	1.85

<sup>a</sup> Molar ratio of HEMA/L-LA/ $\epsilon$ -CL = 1/5/4, 0.5 mol% (based on the monomer) *rac*-BNPH as catalyst, *t* = 7 h. <sup>b</sup> The retention percentage of HEMA terminal vinyl groups in MMs. <sup>c</sup> Molar fraction of monomers in macromonomers determined from <sup>1</sup>H NMR spectra. <sup>d</sup> 0.1 mol% (based on the monomers) peroxybenzene added as inhibitor.

Conversions for L-LA,  $\epsilon$ -CL and overall monomers (*X*) as a function of polymerization time are plotted in Fig. 1a–c. The information on MMs including cumulative L-LA composition (*F*<sub>L</sub>), *M*<sub>n</sub>, and *D* are plotted as a function of overall monomer conversion in Fig. 1d and e. For batch reactions promoted with Sn(Oct)<sub>2</sub>, the L-LA is converted at a higher rate compared with the  $\epsilon$ -CL comonomer. Batch polymerizations catalyzed with *rac*-BNPH demonstrate a more rapid conversion of  $\epsilon$ -CL relative to L-LA. Regulating the  $\epsilon$ -CL feed rates (at 0.0468 and 0.0187 mol h<sup>-1</sup>) in the *rac*-BNPH-catalyzed ROCoPs slows down the  $\epsilon$ -CL polymerization rate in favor of more L-LA incorporated into MM chains. The benefits of this approach are evident in the composition of generated MMs. For batch processes, the *F*<sub>L</sub> in MM deviated substantially from the design value regardless of which catalyst, Sn(Oct)<sub>2</sub> or *rac*-BNPH, was used (see Fig. 1d). Even at overall monomer conversions of greater than 60%, large deviations in comonomer composition exist. The MMs generated using the semibatch process are more homogeneous. The MM *F*<sub>L</sub> values are close to design values with regulated  $\epsilon$ -CL feeding, even at the low monomer conversions. The *M*<sub>n</sub> values of the MMs prepared using all of the various approaches catalyzed with *rac*-BNPH increased linearly with *X*, and all *D* values were held below 1.4, showing living polymerization characteristics. The slightly higher *D* values at high conversions are attributed to the increase of bulk viscosity inhibiting diffusion of monomers.<sup>43</sup>

### Analysis of MM chain structure

Intuitively, the polymerization kinetic behavior described above would be expected to provide MMs possessing a L-LA rich block near the HEMA head group when Sn(Oct)<sub>2</sub> is used as the catalyst in batch operations, while a block of L-LA would be expected to

terminate the MM chain for batch ROCoPs catalyzed with *rac*-BNPH. The <sup>1</sup>H NMR spectra of the  $\epsilon$ - and  $\alpha$ -methylenes and protons adjacent to the terminal hydroxyl group in MMs generated using *rac*-BNPH under batch and semibatch conditions as well as spectra generated using Sn(Oct)<sub>2</sub> under batch conditions are shown in Fig. 2 along with peak assignments for MMs. Full spectra for all of the generated MMs are provided as part of the ESI (Fig. S1†). The reference MMs, L-LA homo-macromonomer with five lactidyl units (LA<sub>5</sub>-HEMA),  $\epsilon$ -CL homo-macromonomer having four  $\epsilon$ -CL units (CL<sub>4</sub>-HEMA), and a block macromonomer of  $\epsilon$ -CL and L-LA using HEMA as initiator (LA<sub>5</sub>-*b*-CL<sub>4</sub>-HEMA) were generated using Sn(Oct)<sub>2</sub> as catalyst. These acted as references to establish chemical shifts that provide the local sequence for the LA and CL units in the formed copolymers. The details for their preparation and peak assignments of <sup>1</sup>H NMR spectra are provided in the ESI (Fig. S2†).

From all four spectra shown in Fig. 2, the triple peak of terminal HO-C around 3.61–3.69 ppm could not be observed clearly, but peaks around 4.4 ppm associated the HO-L end-group are easily distinguishable. The results are consistent with what is expected for the MMs catalyzed with *rac*-BNPH, but it is not statistically consistent with the ROCoP catalyzed with Sn(Oct)<sub>2</sub> in which the  $\epsilon$ -CL is incorporated slowly. The results suggest the presence of TSRs in which the terminal active caproyl end from a MM chain acts as the nucleophile and attacks a carbonyl group located on an adjacent MM chain in the Sn(Oct)<sub>2</sub> catalyzed ROCoP.<sup>44–47</sup> It has been reported that the HO-C end is significantly more active in such reactions compared with a HO-L end-group.<sup>4</sup> Thus, when the MM is synthesized using the *rac*-BNPH catalyst in the batch mode, a long blocky L-LA would be expected at the end of the MM. This is confirmed from the chemical shift of HO-L changing from 4.39–4.48 ppm

Table 3 Data for bulk ROCoP of L-LA and  $\epsilon$ -CL initiated with HEMA using batch and semibatch processes<sup>a</sup>

Run	Catalyst	<i>v</i> <sub>CL</sub> (mol h <sup>-1</sup> )	<i>x</i> <sub>LA</sub> (%)	<i>x</i> <sub>CL</sub> (%)	<i>R</i> <sub>v</sub> <sup>b</sup> (%)	HEMA/L-LA/ $\epsilon$ -CL <sup>c</sup>	<i>M</i> <sub>n</sub> <sup>NMR</sup> (kg mol <sup>-1</sup> )	<i>M</i> <sub>n</sub> <sup>GPC</sup> (kg mol <sup>-1</sup> )	<i>D</i> <sup>GPC</sup>
B8	Sn(Oct) <sub>2</sub>	—	~100	~100	97	1/10.07/4.31	1.35	2.01	1.60
B5 <sup>d</sup>	<i>rac</i> -BNPH	—	92.7	~100	96	1/9.20/4.28	1.28	1.44	1.43
SB1 <sup>d</sup>	<i>rac</i> -BNPH	0.0468	96.0	~100	97	1/9.74/4.62	1.35	1.83	1.38
SB2 <sup>d</sup>	<i>rac</i> -BNPH	0.0187	98.0	~100	~100	1/9.46/4.33	1.30	1.79	1.41

<sup>a</sup> Molar ratio of HEMA/L-LA/ $\epsilon$ -CL = 1/5/4, 0.5 mol% (based on the monomer) catalyst, *t* = 7 h, *T* = 140 °C. <sup>b</sup> Retention percentage of terminal vinyl groups in MMs. <sup>c</sup> Molar fraction of monomers in macromonomers determined from <sup>1</sup>H NMR spectra. <sup>d</sup> 0.1 mol% (based on monomers) peroxybenzene added as inhibitor.





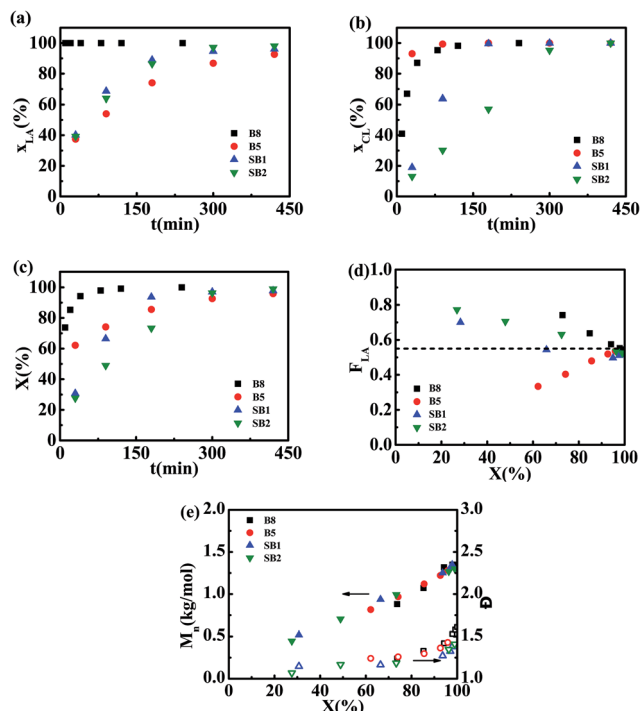


Fig. 1 Bulk ROP of L-LA and ε-CL carried out at 140 °C using a molar ratio of HEMA/L-LA/ε-CL = 1/5/4 with different catalysts and monomer addition modes (B8: Sn(Oct)<sub>2</sub>, batch; B5: *rac*-BNPH, batch; SB1: *rac*-BNPH, semibatch with  $v_{CL} = 0.0468 \text{ mol h}^{-1}$ ; and SB2: *rac*-BNPH, semibatch with  $v_{CL} = 0.0187 \text{ mol h}^{-1}$ ). Shown are results for (a) conversion of L-LA ( $x_{LA}$ ) versus polymerization time (t), (b) conversion of ε-CL ( $x_{CL}$ ) versus t, (c) total conversion of monomers (X) versus t, (d) cumulative molar fraction of L-LA in copolymer ( $F_{LA}$ ) versus X, and (e)  $M_{n,NMR}$  and Đ versus X.

in Runs B8, SB1 and SB2 to 4.35–4.41 ppm in Run B5, which is consistent with the chemical shifts shown for sample LA<sub>5</sub>-HEMA in the ESI (Fig. S2†).

To further parse the MM chain structure for the various reaction conditions, <sup>13</sup>C NMR analysis was employed. The carbonyl carbon peaks between 165 and 175 ppm of the <sup>13</sup>C NMR spectra were the main focus of this analysis. These regions of the spectra and sequential assignments of each peak for the MMs generated *via* the different synthesis approaches are shown in Fig. 3. The <sup>13</sup>C NMR analysis for MMs LA<sub>5</sub>-HEMA, CL<sub>4</sub>-HEMA, and LA<sub>5</sub>-*b*-CL<sub>4</sub>-HEMA was also carried out. Their <sup>13</sup>C NMR spectra and triad assignments are given in Fig. S3 in the ESI.† Here LL is used to denote the lactidyl unit while C is for

and is confirmed by the results of the reference MMs presented in the ESI.†

The peaks at 173.13 and 173.21 ppm from MMs generated in Run B5 (Fig. 3) correspond to the triad of CC-HEMA head groups of MMs prepared by *rac*-BNPH catalyzed batch ROP of L-LA and ε-CL with HEMA initiator. Approximately 75% of formed MMs were initiated *via* reaction between HEMA and ε-CL in the *rac*-BNPH catalyzed batch ROP, while 25% involved reactions between HEMA and L-LA, which is indicated by the peaks at peaks of 169.79 and 169.98 ppm corresponding to the triad of LL-HEMA. These results along with proton NMR spectra strongly suggest the rapid initial addition of ε-CL for these reaction conditions. By changing the operation from a batch to semibatch process through ε-CL metering, the percentages of HEMA initially incorporated with ε-CL dropped to approximately 30% in both Runs SB1 and SB2 corresponding to ε-CL feed rates of 0.0468 and 0.0187 mol h<sup>-1</sup>, respectively. In comparison, almost all of the HEMA was initially reacted with L-LA in Sn(Oct)<sub>2</sub> catalyzed batch ROP of L-LA and ε-CL. The absence of peak corresponding to HO-CC at 173.75 ppm in all MMs further verifies the observation of the MMs possessing terminal HO-LL groups in the <sup>1</sup>H NMR measurement.

The presence of TSRs during Sn(Oct)<sub>2</sub> catalyzed ROP of L-LA and ε-CL has been reported previously.<sup>18</sup> The resonances of CLC triad at 170.83 ppm and CLLC at 169.65 ppm for Run B8 shown in Fig. 3, indicating the presence of an odd number of lactidyl units (L), are evidence of the presence of such reactions. For polymerizations catalyzed with *rac*-BNPH these peaks become indistinguishable for reaction runs under batch mode (Run B5) and semibatch mode using the higher ε-CL feed rate (Run SB1), but becomes slightly noticeable at the lower ε-CL feed rate (Run SB2). For a clearer assessment of the extent to which TSRs are present during ROPs, the percentage of lactyl units (L) present in the MMs, denoted here as  $P_{Trans}$ , was determined by comparing the <sup>13</sup>C NMR spectral area  $A$  associated with sequences possessing these units with the total area associated with sequences having both lactyl and lactidyl units (eqn (1)). The  $P_{Trans}$  value is 20.2% when polymerizations are catalyzed with Sn(Oct)<sub>2</sub> under batch reaction conditions. This value sharply declines to 0% for *rac*-BNPH catalyzed batch and semibatch reactions using the higher ε-CL feed rate in Run SB1, and 2.6% for *rac*-BNPH catalyzed semibatch reaction conditions used in Run SB2. This suggests the TSRs can be suppressed in the *rac*-BNPH catalyzed ROP by controlling the ε-CL concentration in the system.

$$P_{Trans} = \frac{1}{2} \left( \frac{A_{CLC} + A_{CLLC}}{A_{LLLLL} + A_{CLLC} + A_{LLLLL} + A_{CLLLL} + A_{CLC} + A_{CLLC}} + \frac{A_{CLCC} + A_{CLCLC} + A_{CLLCL}}{A_{CCC} + A_{LLCLL} + A_{LLCC} + A_{CCLL} + A_{CLCC} + A_{CLCLC} + A_{CLLCL}} \right) \quad (1)$$

carboxyl unit. All peak assignments in the figure are consistent with those reported by Kasperczyk and Bero,<sup>48</sup> with the exception of chemical shifts 170.32 and 170.08 ppm, which were assigned to sequences LLLC and CLLL, respectively. This is the opposite of the previously reported assignments in ref. 48,

The sequential distribution in the MMs is further investigated through the triad distribution and average sequence length of each monomer unit. Since there exist lactyl units in some MM samples, the triads and average sequence lengths on the basis of lactyl unit L are considered. The triad *ijk*

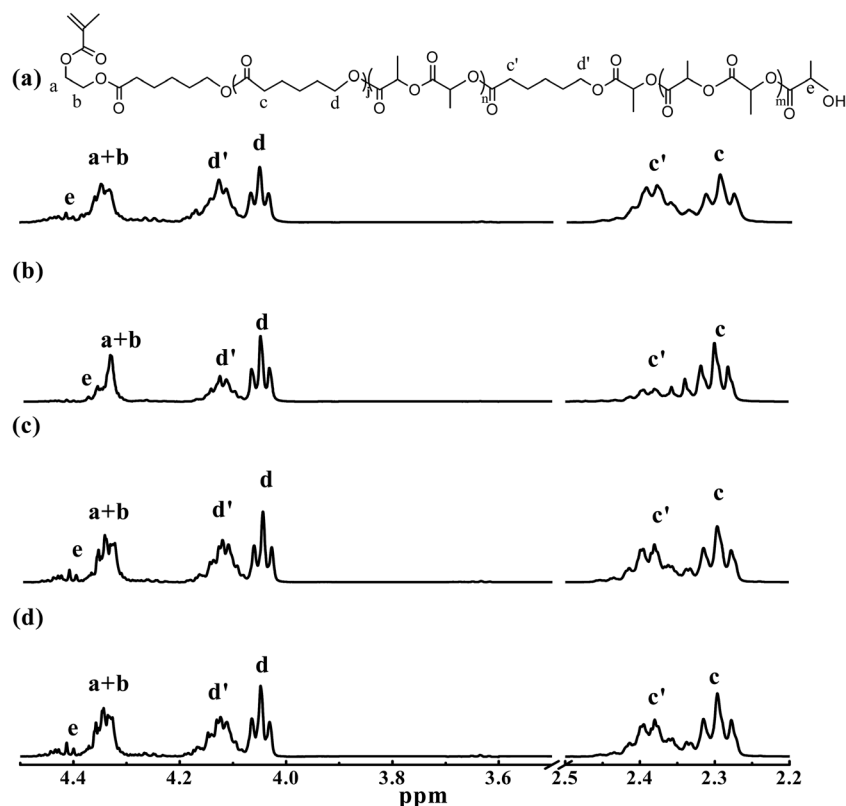


**Fig. 2**  $^1\text{H}$  NMR spectra of the  $\varepsilon$ - and  $\alpha$ -methylenes and protons adjacent to terminal hydroxyl group in macromonomers. Shown are  $^1\text{H}$  NMR spectra for (a) B8:  $\text{Sn}(\text{Oct})_2$ , batch; (b) B5: *rac*-BNPH, batch; (c) SB1: *rac*-BNPH, semibatch with  $v_{\text{CL}} = 0.0468 \text{ mol h}^{-1}$ ; and (d) SB2: *rac*-BNPH, semibatch with  $v_{\text{CL}} = 0.0187 \text{ mol h}^{-1}$ .

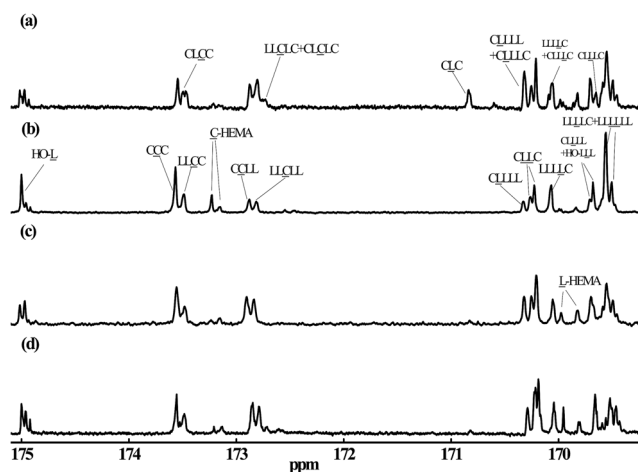


**Fig. 3** Carbonyl carbon regions of  $^{13}\text{C}$  NMR spectra for MMs produced through different synthesis approaches. Shown are  $^{13}\text{C}$  NMR spectra for (a) B8, batch and  $\text{Sn}(\text{Oct})_2$  catalyzed, (b) B5, batch and *rac*-BNPH catalyzed, (c) SB1, semibatch with  $v_{\text{CL}} = 0.0468 \text{ mol h}^{-1}$  and *rac*-BNPH catalyzed, and (d) SB2, semibatch with  $v_{\text{CL}} = 0.0187 \text{ mol h}^{-1}$  and *rac*-BNPH catalyzed.

distributions ( $P(\text{ijk})$ ) in the MMs can be estimated from Fig. 3. The relationships between the triad distributions and the integral areas in the  $^{13}\text{C}$  NMR spectra are<sup>49</sup>

$$P(\text{LLL}) = k \left( \frac{1}{2} A_{\text{CLLLL}} + \frac{1}{2} A_{\text{LLLLC}} + \frac{1}{3} A_{\text{CLLLC}} + A_{\text{LLLLL}} \right) \quad (2)$$

$$P(\text{LLC}) = k \left( \frac{1}{2} A_{\text{CLLC}} + \frac{1}{2} A_{\text{LLLLC}} + \frac{1}{3} A_{\text{CCLLC}} \right) \quad (3)$$

$$P(\text{CLL}) = k \left( \frac{1}{2} A_{\text{CLLC}} + \frac{1}{2} A_{\text{CLLLL}} + \frac{1}{3} A_{\text{CLLLC}} \right) \quad (4)$$

$$P(\text{CLC}) = kA_{\text{CLC}} \quad (5)$$

$$P(\text{LCL}) = k(A_{\text{LLCLL}} + A_{\text{LLCLC}} + A_{\text{CLCLL}} + A_{\text{CLCLC}}) \quad (6)$$

$$P(\text{CCL}) = k(A_{\text{CCLC}} + A_{\text{CCLL}}) \quad (7)$$

$$P(\text{LCC}) = k(A_{\text{CLCC}} + A_{\text{LLCC}}) \quad (8)$$

$$P(\text{CCC}) = kA_{\text{CCC}} \quad (9)$$

where  $k$  is the NMR signal proportionality constant.

The triad distributions for the MMs are summarized in Table 4. For the batch copolymerization Run B5 using *rac*-BNPH as the catalyst, more CCC and LLL triads were identified compared to that found in Run B8 with Sn(Oct)<sub>2</sub> as the catalyst. In comparing Run B5 with *rac*-BNPH catalyzed semibatch reactions at the lowest  $\epsilon$ -CL feed rate (SB2), the CCC sequence

**Table 4** Triad distributions in macromonomers synthesized in HEMA initiated bulk ROCoP of L-LA and ε-CL catalyzed by either *rac*-BNPH or Sn(Oct)<sub>2</sub>

Triad distribution	B8	B5	SB1	SB2
<i>P</i> (CCC)	0.090	0.231	0.186	0.129
<i>P</i> (CCL)	0.087	0.088	0.148	0.150
<i>P</i> (LCC)	0.101	0.125	0.083	0.114
<i>P</i> (LCL)	0.187	0.076	0.116	0.129
<i>P</i> (CLC)	0.076	0.000	0.000	0.010
<i>P</i> (LLC)	0.099	0.116	0.120	0.149
<i>P</i> (CLL)	0.099	0.068	0.123	0.126
<i>P</i> (LLL)	0.261	0.297	0.224	0.194

distributions decrease from 0.231 to 0.129, respectively, while the LLL sequences decrease from 0.297 to 0.194, respectively. This is accompanied by an increase in the CCL, LCL, LLC, and CLL sequences, suggesting more uniformly distributed comonomer sequential structures in the MMs due to slow addition of ε-CL. The triad distributions except CLC, which is contributed by the TSR, in Run SB2 are similar.

From the triad distribution data, the average sequence lengths of lactyl and caproyl units,  $\bar{l}_L^e$  and  $\bar{l}_C^e$ , respectively, in the MMs can be estimated using,

$$\bar{l}_L^e = \frac{P(\text{LLL}) + P(\text{CLL}) + P(\text{LLC}) + P(\text{CLC})}{P(\text{CLC}) + \frac{1}{2}(P(\text{LLC}) + P(\text{CLL}))} \quad (10)$$

$$\bar{l}_C^e = \frac{P(\text{CCC}) + P(\text{LCL}) + P(\text{LCC}) + P(\text{CCL})}{P(\text{LCL}) + \frac{1}{2}(P(\text{CCL}) + P(\text{LCC}))} \quad (11)$$

The results of average sequence lengths of lactyl and caproyl units are summarized in Table 5. The evidence of  $\bar{l}_L^e$  and  $\bar{l}_C^e$  becoming shorter with the change of ε-CL feed strategy from batch mode to slow addition of ε-CL is further observed. Run SB2 by *rac*-BNPH catalyzed semibatch ROCoP with slowest ε-CL addition has  $\bar{l}_L^e$  and  $\bar{l}_C^e$  values close to those in Run B8 by Sn(Oct)<sub>2</sub> catalyzed batch reaction, suggesting the MM sequential structures become more random. The semibatch operation with ε-CL addition is an effective means for tailoring the MMs with more uniformly distributed comonomer sequential structures.

**Table 5** Average sequence lengths of lactyl and caproyl units in macromonomers synthesized in HEMA initiated bulk ROCoP of L-LA and ε-CL catalyzed by either *rac*-BNPH or Sn(Oct)<sub>2</sub> using batch and semibatch processes

Run	$\bar{l}_L^e$	$\bar{l}_C^e$
B8	3.06	1.65
B5	5.22	2.85
SB1	3.84	2.30
SB2	3.25	2.00

## Conclusions

The first successful catalysis of HEMA initiated ROCoPs of L-LA and ε-CL using *rac*-BNPH is reported. Narrowly dispersed MMs with a 96% retention of HEMA terminal vinyl groups were generated at 140 °C using 0.5 mol% catalyst and 0.1 mol% inhibitor and a HEMA/L-LA/ε-CL molar ratio of 1/5/4. It was observed that when *rac*-BNPH is applied, ε-CL is more reactive than L-LA, which is the opposite to the reactivity order observed when using Sn(Oct)<sub>2</sub> as the catalyst. The ROCoP showed living characteristics. Using semibatch operation involving the regulation of ε-CL feed rates to 0.0468 and 0.0187 mol h<sup>-1</sup> generated MMs with more homogeneous comonomer compositions. The <sup>1</sup>H and <sup>13</sup>C NMR characterization results showed that the MMs prepared with *rac*-BNPH possess terminal OH-LA units. It was also found that 75% of MMs generated *via* batch reactions have initial CL-HEMA groups, which dropped to 30% for semibatch reactions. The prevalence of TSRs was greatly reduced when these reactions are catalyzed with *rac*-BNPH and ε-CL feed rates are controlled. No TSRs were observed in *rac*-BNPH catalyzed batch and semibatch reactions using the higher ε-CL feed rate. Approximately 2.6% lactyl units participated in the TSRs during *rac*-BNPH catalyzed semibatch ROCoPs using the lower feed rate of 0.0187 mol h<sup>-1</sup>, which is significantly lower than the 20.2% lactyl unit participation measured during batch copolymerization using Sn(Oct)<sub>2</sub> as the catalyst. By moving from batch mode to slow addition of ε-CL in *rac*-BNPH catalyzed ROCoPs, both CCC and LLL sequence distributions in the MMs were decreased, and the comonomer sequential structures became more uniformly distributed and random in the MMs. In summary, it was shown that *rac*-BNPH catalyzed ROCoPs with ε-CL addition is an effective means for tailoring the comonomer sequential structures of the MMs.

## Author contributions

The manuscript was written with contributions of all authors. All authors have given approval to the final version of the manuscript.

## Acknowledgements

The authors thank National Key Research and Development Program of China (2016YFB0302402 and 2016YFB0302405), National Natural Science Foundation of China (21420102008), and Chinese State Key Laboratory of Chemical Engineering at Zhejiang University (SKL-ChE-15D03) for financial supports.

## References

- 1 L. Shen, E. Worrell and M. Patel, Present and Future Development in Plastics from Biomass, *Biofuels, Bioprod. Biorefn.*, 2010, **4**, 25–40.
- 2 T. Iwata, Biodegradable and Bio-Based Polymers: Future Prospects of Eco-Friendly Plastics, *Angew. Chem., Int. Ed.*, 2015, **54**, 3210–3215.



- 3 K. Sudesh and T. Iwata, Review: Sustainability of Biobased and Biodegradable Plastics, *Clean*, 2008, **36**, 433–442.
- 4 Z. Y. Wei, L. Liu, C. Qu and M. Qi, Microstructure Analysis and Thermal Properties of L-Lactide/ $\epsilon$ -Caprolactone Copolymers Obtained with Magnesium Octoate, *Polymer*, 2009, **50**, 1423–1429.
- 5 K. Ishimoto, M. Arimoto, H. Ohara, S. Kobayashi, M. Ishii, K. Morita, H. Yamashita and N. Yabuuchi, Biobased Polymer System: Miniemulsion of Poly(alkyl methacrylate-graft-lactic acid)s, *Biomacromolecules*, 2009, **10**, 2719–2723.
- 6 G. Pu, D. A. Hauge, C. Gu, J. Zhang, S. J. Severtson, W. Wang and C. J. Houtman, Influence of Acrylated Lactide-Caprolactone Macromonomers on the Performance of High Biomass Content Pressure-Sensitive Adhesives, *Macromol. React. Eng.*, 2013, **7**, 515–526.
- 7 K. Ishimoto, M. Arimoto, T. Okuda, S. Yamaguchi, Y. Aso, H. Ohara, S. Kobayashi, M. Ishii, K. Morita, H. Yamashita and N. Yabuuchi, Biobased Polymers: Synthesis of Graft Copolymers and Comb Polymers Using Lactic Acid Macromonomer and Properties of the Product Polymers, *Biomacromolecules*, 2012, **13**, 3757–3768.
- 8 T. Okuda, K. Ishimoto, H. Ohara and S. Kobayashi, Renewable Biobased Polymeric Materials: Facile Synthesis of Itaconic Anhydride-Based Copolymers with Poly(L-lactic acid) Grafts, *Macromolecules*, 2012, **45**, 4166–4174.
- 9 X. Liu and P. X. Ma, The Nanofibrous Architecture of Poly(L-lactic acid)-Based Functional Copolymers, *Biomaterials*, 2010, **31**, 259–269.
- 10 G. Pu, M. R. Dubay, J. Zhang and S. J. Severtson, Polyacrylates with High Biomass Contents for Pressure-Sensitive Adhesives Prepared via Mini-emulsion Polymerization, *Ind. Eng. Chem. Res.*, 2012, **51**, 12145–12149.
- 11 C. Gu, M. R. Dubay and S. J. Severtson, Hot-Melt Pressure-Sensitive Adhesives Containing High Biomass Contents, *Ind. Eng. Chem. Res.*, 2014, **53**, 11000–11006.
- 12 P. Kurock, M. Kowalczyk, K. Hennek and Z. Jedlinski, Anionic Polymerization of Lactones Initiated with Alkali-Metal Alkoxides: Reinvestigation of the Polymerization Mechanism, *Macromolecules*, 1992, **25**, 2017–2020.
- 13 O. Dechy-Cabaret, B. Martin-Vaca and D. Bourissou, Controlled Ring-Opening Polymerization of Lactide and Glycolide, *Chem. Rev.*, 2004, **104**, 6147–6176.
- 14 C. M. Thomas, Stereocontrolled Ring-Opening Polymerization of Cyclic Esters: Synthesis of New Polyester Microstructures, *Chem. Soc. Rev.*, 2010, **39**, 165–173.
- 15 P. J. Dijkstra, H. Z. Du and F. J. Jan, Single Site Catalysts for Stereoselective Ring-Opening Polymerization of Lactides, *Polym. Chem.*, 2011, **2**, 520–527.
- 16 L. Zhang, F. Nederberg, R. C. Pratt, R. M. Waymouth, J. L. Hedrick and C. G. Wade, Phosphazene Bases: A New Category of Organocatalysts for the Living Ring-Opening Polymerization of Cyclic Esters, *Macromolecules*, 2007, **40**, 4154–4158.
- 17 E. F. Connor, G. W. Nyce, M. Myers, A. Möck and J. L. Hedrick, First Example of N-Heterocyclic Carbenes as Catalysts for Living Polymerization: Organocatalytic Ring-Opening Polymerization of Cyclic Esters, *J. Am. Chem. Soc.*, 2002, **124**, 914–915.
- 18 H. R. Kricheldorf, M. Berl and N. Scharnagl, Poly(lactones). 9. Polymerization Mechanism of Metal Alkoxide Initiated Polymerizations of Lactide and Various Lactones, *Macromolecules*, 1988, **21**, 286–293.
- 19 M. K. Kiesewetter, E. J. Shin, J. L. Hedrick and R. M. Waymouth, Organocatalysis: Opportunities and Challenges for Polymer Synthesis, *Macromolecules*, 2010, **43**, 2093–2107.
- 20 Y. Miao, Y. Phuphuak, C. Rousseau, T. Bousquet, A. Mortreux, S. Chirachanchai and P. Zinck, Ring-Opening Polymerization of Lactones using Binaphthyl-diyl Hydrogen Phosphate as Organocatalyst and Resulting Monosaccharide Functionalization of Poly(lactones), *J. Polym. Sci., Part A: Polym. Chem.*, 2013, **51**, 2279–2287.
- 21 X. Zhou and L. Z. Hong, Controlled Ring-Opening Polymerization of Cyclic Esters with Phosphoric Acid as Catalysts, *Colloid Polym. Sci.*, 2013, **291**, 2155–2162.
- 22 S. Wang, P. Liu, W.-J. Wang, Z. Zhang and B.-G. Li, Hyperbranched Polyethylene-Supported L-proline: A Highly Selective and Recyclable Organocatalyst for Asymmetric Aldol Reactions, *Catal. Sci. Technol.*, 2015, **5**, 3798–3805.
- 23 T. Endo, Y. Shibasaki and F. Sanda, Controlled Ring-Opening Polymerization of Cyclic Carbonates and Lactones by An Activated Monomer Mechanism, *J. Polym. Sci., Part A: Polym. Chem.*, 2002, **40**, 2190–2198.
- 24 G.-B. Stéphanie, D. Damien, M.-V. Blanca, B. Didier, N. Christophe and M. Stéphanie, Organo-Catalyzed ROP of  $\epsilon$ -Caprolactone: Methanesulfonic Acid Competes with Trifluoromethanesulfonic Acid, *Macromolecules*, 2008, **41**, 3782–3784.
- 25 N. Susperregui, D. Delcroix, B. Martinvaca, D. Bourissou and L. Maron, Ring-Opening Polymerization of  $\epsilon$ -Caprolactone Catalyzed by Sulfonic Acids: Computational Evidence for Bifunctional Activation, *J. Org. Chem.*, 2010, **75**, 6581–6587.
- 26 S. Boileau and N. Illy, Activation in Anionic Polymerization: Why Phosphazene Bases Are Very Exciting Promoters, *Prog. Polym. Sci.*, 2011, **36**, 1132–1151.
- 27 G. Mountrichas, C. Mantzaridis and S. Pispas, Well-Defined Flexible Polyelectrolytes with Two Cationic Sites per Monomeric Unit, *Macromol. Rapid Commun.*, 2006, **27**, 289–294.
- 28 C. G. Wade and J. L. Hedrick, Organocatalytic Stereoselective Ring-Opening Polymerization of Lactide with Dimeric Phosphazene Bases, *J. Am. Chem. Soc.*, 2007, **129**, 12610–12611.
- 29 M. Fevre, J. Pinaud, Y. Gnanou, J. Vignolle and D. Taton, N-Heterocyclic Carbenes (NHCs) as Organocatalysts and Structural Components in Metal-free Polymer Synthesis, *Chem. Soc. Rev.*, 2013, **42**, 2142–2172.
- 30 J. Raynaud, C. Absalon, Y. Gnanou and D. Taton, N-Heterocyclic Carbene-Organocatalyzed Ring-Opening Polymerization of Ethylene Oxide in the Presence of Alcohols or Trimethylsilyl Nucleophiles as Chain Moderators for the Synthesis of  $\alpha,\omega$ -Heterodifunctionalized Poly(ethylene oxide)s, *Macromolecules*, 2010, **43**, 2814–2823.





- 31 J. Raynaud, C. Absalon, Y. Gnanou and D. Taton, N-Heterocyclic Carbene-Induced Zwitterionic Ring-Opening Polymerization of Ethylene Oxide and Direct Synthesis of  $\alpha,\omega$ -Difunctionalized Poly(ethylene oxide)s and Poly(ethylene oxide)-*b*-poly( $\epsilon$ -caprolactone) Block Copolymers, *J. Am. Chem. Soc.*, 2009, **131**, 3201–3209.
- 32 B. G. G. Lohmeijer, R. C. Pratt, F. Leibfarth, J. W. Logan, D. A. Long, A. P. Dove, F. Nederberg, J. Choi, C. Wade, R. M. Waymouth and J. L. Hedrick, Guanidine and Amidine Organocatalysts for Ring-Opening Polymerization of Cyclic Esters, *Macromolecules*, 2006, **39**, 8574–8583.
- 33 A. P. Dove, R. C. Pratt, B. G. G. Lohmeijer, R. M. Waymouth and J. L. Hedrick, Thiourea-Based Bifunctional Organocatalysis: Supramolecular Recognition for Living Polymerization, *J. Am. Chem. Soc.*, 2005, **127**, 13798–13799.
- 34 M. Oshimura, T. Tang and A. Takasu, Ring-opening Polymerization of  $\epsilon$ -Caprolactone Using Perfluoroalkanesulfonates and Perfluoroalkanesulfonimides as Organic Catalysts, *J. Polym. Sci., Part A: Polym. Chem.*, 2011, **49**, 1210–1218.
- 35 F. Nederberg, E. F. Connor, M. Möller, T. Glauser and J. L. Hedrick, New Paradigms for Organic Catalysts: The First Organocatalytic Living Polymerization, *Angew. Chem., Int. Ed.*, 2001, **40**, 2712–2715.
- 36 D. A. Culkin, W. Jeong, S. Csihony, E. D. Gomez, N. P. Balsara, J. L. Hedrick and R. M. Waymouth, Zwitterionic Polymerization of Lactide to Cyclic Poly(Lactide) by Using N-Heterocyclic Carbene Organocatalysts, *Angew. Chem., Int. Ed.*, 2007, **119**, 2681–2684.
- 37 M. L. Foresti and M. L. Ferreira, Synthesis of Polycaprolactone Using Free/Supported Enzymatic and Non-Enzymatic Catalysts, *Macromol. Rapid Commun.*, 2004, **25**, 2025–2028.
- 38 R. C. Pratt, B. G. G. Lohmeijer, D. A. Long, R. M. Waymouth and J. L. Hedrick, Triazabicyclodecene: A Simple Bifunctional Organocatalyst for Acyl Transfer and Ring-Opening Polymerization of Cyclic Esters, *J. Am. Chem. Soc.*, 2006, **128**, 4556–4557.
- 39 G. Theryo, F. Jing, L. M. Pitet and M. A. Hillmyer, Tough Polylactide Graft Copolymers, *Macromolecules*, 2010, **43**, 7394–7397.
- 40 S. Jaenicke, G. K. Chuah, X. H. Lin and X. C. Hu, Organic-inorganic Hybrid Catalysts for Acid- and Base-catalyzed Reactions, *Microporous Mesoporous Mater.*, 2000, **99**, 143–153.
- 41 F. Suriano, O. Coulembier, J. L. Hedrick and P. Dubois, Functionalized Cyclic Carbonates: from Synthesis and Metal-free Catalyzed Ring-opening Polymerization to Applications, *Polym. Chem.*, 2011, **2**, 528–533.
- 42 G. W. Nyce, T. Glauser, E. F. Connor, A. Möck, R. M. Waymouth and J. L. Hedrick, *In Situ* Generation of Carbenes: A General and Versatile Platform for Organocatalytic Living Polymerization, *J. Am. Chem. Soc.*, 2003, **125**, 3046–3056.
- 43 F. Y. Weng, X. H. Li, Y. J. Wang, W.-J. Wang and S. J. Severtson, Kinetics and Modeling of Ring-Opening Copolymerization of L-Lactide and  $\epsilon$ -Caprolactone, *Macromol. React. Eng.*, 2015, **9**, 535–544.
- 44 M. Bero and J. Kasperczyk, Coordination Polymerization of Lactides, 5. Influence of Lactide Structure on the Transesterification Processes in the Copolymerization with  $\epsilon$ -Caprolactone, *Macromol. Chem. Phys.*, 1996, **197**, 3251–3258.
- 45 A. Kowalski, A. Duda and S. Penczek, Kinetics and Mechanism of Cyclic Esters Polymerization Initiated with Tin(II) Octoate, 1. Polymerization of  $\epsilon$ -Caprolactone, *Macromol. Rapid Commun.*, 1998, **19**, 567–572.
- 46 A. Kowalski, A. Duda and S. Penczek, Mechanism of Cyclic Ester Polymerization Initiated with Tin(II) Octoate. 2. Macromolecules Fitted with Tin(II) Alkoxide Species Observed Directly in MALDI-TOF Spectra, *Macromolecules*, 2000, **33**, 689–695.
- 47 A. Kowalski, A. Duda and S. Penczek, Kinetics and Mechanism of Cyclic Esters Polymerization Initiated with Tin(II) Octoate. 3. Polymerization of L,L-Dilactide, *Macromolecules*, 2000, **33**, 7359–7370.
- 48 J. Kasperczyk and M. Bero, Coordination Polymerization of Lactides, 2. Microstructure Determination of Poly([L,L-lactide)-co-( $\epsilon$ -caprolactone)] with  $^{13}\text{C}$  Nuclear Magnetic Resonance Spectroscopy, *Makromol. Chem.*, 1991, **192**, 1777–1787.
- 49 J. Kasperczyk and M. Bero, Coordination Polymerization of Lactides, 4. The Role of Transesterification in the Copolymerization of L,L-lactide and  $\epsilon$ -Caprolactone, *Makromol. Chem.*, 1993, **194**, 913–925.

